Small-Angle Neutron Scattering and Theoretical Investigation of Poly(ethylene oxide)−Poly(propylene oxide)−Poly(ethylene oxide) Stabilized Oil-in-Water Microemulsions

John S. Lettow,[†] Thomas M. Lancaster,[†] Charles J. Glinka,[‡] and Jackie Y. Ying*[,†,§]

Department of Chemical Engineering, Massachusetts Institute of Technology, Cambridge, Massachusetts 02139, Cold Neutron Research Facility, National Institute of Standards and Technology, Gaithersburg, Maryland 20899, and Institute of Bioengineering and Nanotechnology, 31 Biopolis Way, The Nanos, Singapore 138669

Received December 15, 2004. In Final Form: March 25, 2005

The aim of this study is to determine the effects of oil solutes and alcohol cosolvents on the structure of oil-in-water microemulsions stabilized by poly(ethylene oxide)−poly(propylene oxide)−poly(ethylene oxide) (PEO−PPO−PEO) triblock copolymers. The systems investigated involved the solubilization of 1,3,5-trimethylbenzene or 1,2-dichlorobenzene by P123 (EO_{20}−PO_{70}−EO_{20}) pluronic surfactant micelles in water and water + ethanol solvents. The structures of these swollen micelles were determined by small-angle neutron scattering (SANS). A thermodynamic model was employed to interpret the characterization data. The results of the thermodynamic model for micellization agreed well with the SANS data from samples of micelles swollen by both oils. The model predicted the size of the micelles within 5% accuracy using only one fitting parameter, the micelle polydispersity. Ethanol had significantly different effects on the polymer micelles that contained solubilized oil compared to pure polymer micelles. For pure polymer micelles, the addition of ethanol increased the solubility of the polymer and, therefore, decreased the total volume fraction of micelles, while for polymer−oil aggregates, ethanol tended to have a positive effect on the volume fraction of micelles. SANS results showed that the greatest divergence from pure aqueous solvent results occurred at oil concentrations above the microemulsion stability limit.

Introduction

Poly(ethylene oxide)−poly(propylene oxide)−poly(ethylene oxide) (PEO−PPO−PEO) triblock copolymers have found application in a wide variety of fields[1] from water remediation[2] to cosmetics[3] and drug delivery.[4,5] Many of these applications depend on the copolymer amphiphile's ability to solubilize hydrophobic compounds, thus, forming polymer aggregates "swollen" by the hydrophobic solute. Alexandridis and co-workers have noted the rich micellar phase behavior of Pluronic (the commercial name for BASF's PEO−PPO−PEO surfactants)−oil−water mixtures.[6,7] Recently, researchers have utilized the phase behavior of PEO−PPO−PEO aggregates to template the formation of inorganic mesostructures[8] and have found that the addition of swelling agents (such as trimethylbenzene) to the polymer micelles results in the formation of a unique inorganic mesophase known as a siliceous mesocellular foam.[9,10] Alcohols play an important role in many of these applications from their presence in self-assembling silica structures due to the hydrolysis of silicon alkoxide precursors to their presence in waste streams and their use in pharmaceutical and cosmetic formulations.

Numerous researchers have tested the macroscopic properties of swollen micellar systems, such as their cloud point,[2,11,12] rheological behavior,[13] and stability in the presence of various cosolvents.[11,14] Other experimentalists have performed detailed studies of the microscopic structure of PEO−PPO−PEO micelles in water using techniques such as dynamic and static light scattering and small-angle X-ray scattering (SAXS), as well as small-angle neutron scattering (SANS).[15−17] Theorists have also

* To whom correspondence should be addressed.
[†] Massachusetts Institute of Technology.
[‡] National Institute of Standards and Technology.
[§] Institute of Bioengineering and Nanotechnology.

(1) Alexandridis, P.; Hatton, T. A. *Colloids Surf., A* **1995**, *96*, 1.
(2) Hurter, P. N.; Alexandridis, P.; Hatton, T. A. In *Solubilization in Surfactant Aggregates*; Christian, S. D., Scamehorn, J. F., Eds.; Marcel Dekker: New York, 1995.
(3) Schmolka, I. R. *Cosmet. Toiletries* **1984**, *99*, 69.
(4) Guzman, M.; Garcia, F. F.; Molpeceres, J.; Aberturas, M. R. *Int. J. Pharm.* **1992**, *80*, 119.
(5) Kabanov, A. V.; Battrakova, E. V.; Melik-Nubarov, N. S.; Fedoseev, N. A.; Dorodnich, T. Y.; Alakhov, V. Y.; Chekhonin, V. P.; Nazalova, I. R.; Kabanov, V. A. *J. Controlled Release* **1992**, *22*, 141.
(6) Alexandridis, P.; Olsson, U.; Lindman, B. *Macromolecules* **1995**, *28*, 7700.
(7) Holmqvist, P.; Alexandridis, P.; Lindman, B. *J. Phys. Chem. B* **1998**, *102*, 1149.
(8) Zhao, D.; Feng, J.; Huo, Q.; Melosh, N.; Fredrickson, G. H.; Chmelka, B. F.; Stucky, G. D. *Science* **1998**, *279*, 548.
(9) Schmidt-Winkel, P.; Lukens, W. W., Jr.; Yang, P.; Margolese, D. I.; Lettow, J. S.; Ying, J. Y.; Stucky, G. D. *Chem. Mater.* **2000**, *12*, 686.
(10) Lettow, J. S.; Han, Y. J.; Schmidt-Winkel, P.; Yang, P.; Zhao, D.; Stucky, G. D.; Ying, J. Y. *Langmuir* **2000**, *16*, 8291.
(11) Pandya, K.; Bahadur, P.; Nagar, T. N.; Bahadur, A. *Colloids Surf.* **1993**, *70*, 219.
(12) Nagarajan, R.; Ganesh, K. *J. Colloid Interface Sci.* **1996**, *184*, 489.
(13) Bahadur, P.; Pandya, K.; Almgren, M.; Li, P.; Stilbs, P. *Colloid Polym. Sci.* **1993**, *271*, 657.
(14) Armstrong, J.; Chowdhry, B.; Mitchell, J.; Beezer, A.; Leharne, S. *J. Phys. Chem.* **1996**, *100*, 1738.
(15) Liu, Y.; Chen, S.-H.; Huang, J. S. *Macromolecules* **1998**, *31*, 6226.
(16) Liu, Y.; Chen, S.-H.; Huang, J. S. *Macromolecules* **1998**, *31*, 2236.
(17) Goldmints, I.; von Gottberg, K.; Smith, K. A.; Hatton, T. A. *Langmuir* **1997**, *13*, 3659.

10.1021/la046918b CCC: $30.25
Published on Web 05/27/2005

turned their attention to Pluronic micelles and oil-swollen micelles, developing models capable of predicting the bulk properties as well as the microscopic structures of the complex fluids.[12,18] However, most experimental studies of oil-swollen Pluronic micelles, even those utilizing powerful scattering techniques such as SAXS and SANS, have taken simplified views of the oil−polymer aggregates by treating them as homogeneous hard spheres or cylinders and have not attempted to confirm the detailed structural predictions of available models.[6,19]

We have compared the results of neutron scattering experiments on Pluronic micelles swollen by two different oils to the predictions of a thermodynamic model for Pluronic−oil aggregate formation first developed by Nagarajan and Ganesh.[12] These experiments achieved three goals: first, they confirmed the accuracy of the model; second, they reduced the neutron scattering fit parameters to a reasonable number, thus, simplifying interpretation of the data; and finally, they result in a more detailed understanding of the major factors contributing to the formation and stability of these important self-assembled mesostructures.

Experimental Procedures

The SANS experiments were performed at the National Institute of Standards and Technology, Gaithersburg, MD, on the 30-m SANS spectrometer, neutron guide NG3. We used neutrons of wavelength $\lambda = 6$ Å with $\Delta\lambda/\lambda = 15\%$ at sample-to-detector distances of 2 and 13 m. This instrument configuration allowed us to cover a range in the magnitude of the wave vector transfer ($|q| = |k_i - k_s| = (4\pi/\lambda) \sin \theta$) from 0.005 to 0.3 Å^{-1}. The neutron intensity was corrected for instrument dark current, empty cell scattering, and beam transmission to obtain an absolute neutron intensity. For all experiments, 1-mm-spaced flat quartz cells were used. The samples were injected into the sample cells at room temperature, and the cells were then placed in the instrument sample chamber and heated to 35 °C. Samples were allowed to equilibrate for several hours before data were taken, and the temperature was controlled within ±0.5 °C.

A typical microemulsion sample was made by first dissolving 0.1 g of PEO−PPO−PEO triblock copolymer (Pluronic P123, $EO_{20}-PO_{70}-EO_{20}$, molecular weight ∼ 5800, BASF) in 10 g of distilled water. To the aqueous polymer solution was slowly added 0−0.1 g of 1,3,5-trimethylbenzene (TMB) or 1,2-dichlorobenzene (DCB; Aldrich). The resulting microemulsion was stirred for several hours and then allowed to equilibrate at room temperature for at least 48 h.

The samples were made at relatively low micelle volume fractions (0.01−0.02) to avoid intermicellar interactions that would complicate the SANS pattern. In addition, two samples were made for each oil concentration: one used a mixture of H_2O and D_2O in the solvent such that the neutron scattering length density (SLD) of the solvent matched that of the polymer (∼5×10^{-7} Å^{-2}) and one in which both the solvent and the oil were mixed with deuterated compounds to increase the contrast between oil, polymer, and solvent.

Model of Microemulsion Structure

The basic structure of a PEO−PPO−PEO triblock copolymer micelle consists of a well-hydrated corona of PEO and a core that contains PPO. Previous SANS studies by Goldmints et al.[17] and Liu et al.[16] have taken slightly different approaches to this "core−shell" model. Although PPO and PEO chains are indistinguishable in neutron scattering due to their nearly identical neutron SLDs, the greater hydration of the PEO chains means that the corona and core regions of PEO−PPO−PEO micelles in water can be clearly identified. Determining the distributions of polymer within these regions, however, is less straightforward. Both Goldmints et al. and Liu et al. have obtained the most accurate fits to neutron scattering data when they included small amounts of water in the PPO core. Both groups used a homogeneous distribution of PPO and water in the micelle core with PPO volume fractions of 80−97%. The PEO corona, on the other hand, contains a significant amount of water, and some researchers have estimated that three water molecules are hydrogen-bonded to each ethylene oxide (EO) unit,[20] and other investigations indicated a total hydration of approximately 20 water molecules per EO unit due to mechanical entrapment.[21] Therefore, the total PEO volume fraction in the corona is 10−40%, assuming a homogeneous distribution of PEO as was assumed by Goldmints et al. Liu et al., however, described the concentration of PEO from the core interface into the solvent with a Gaussian distribution and have obtained accurate fits to neutron scattering data using this model without the need for a micelle polydispersity fitting parameter.[16]

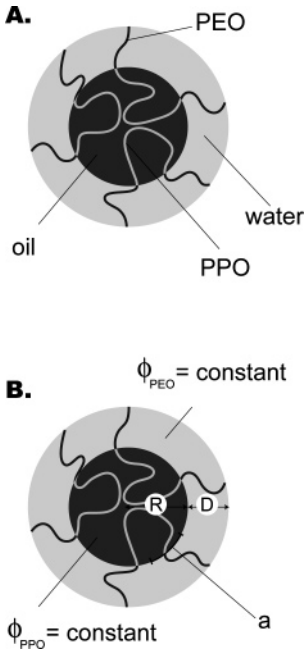

Figure 1. Swollen micelle structure: (A) location of components and (B) important parameters. R is the core radius, D is the corona (or shell) thickness, φ_{PPO} is the volume fraction of PPO in the core that is assumed to be constant, and φ_{PEO} is the volume fraction of PEO in the corona that is also assumed to be constant. Note that, including a micelle polydispersity parameter, there are five variables necessary for describing this simplified swollen micelle model.

To these descriptions of the PEO−PPO−PEO micelles, we now desire to add an oil solubilized in the PPO core. Even if we make the simplifying assumptions that the PPO core contains no water, because it now contains oil, and that PPO and PEO are homogeneously distributed in the core and corona, respectively, we are still left with at least five fitting parameters as shown in Figure 1. We have, therefore, employed a thermodynamic model for the solubilization of hydrocarbons in triblock copolymers developed by Nagarajan and Ganesh to predict the

(18) Hurter, P. N.; Scheutjens, J. M. H. M.; Hatton, T. A. *Macromolecules* **1993**, *26*, 5592.
(19) Schmidt-Winkel, P.; Glinka, C. J.; Stucky, G. D. *Langmuir* **2000**, *16*, 356.
(20) Liu, K.-J.; Parsons, J. L. *Macromolecules* **1969**, *2*, 529.
(21) Nolan, S. L.; Phillips, R. J.; Cotts, P. M.; Dungan, S. R. *J. Colloid Interface Sci.* **1997**, *191*, 291.

microemulsion droplet size and composition, thereby reducing the number of parameters necessary to fit the SANS data.[12,22] The model is based on the "pseudophase" approximation for micelle aggregation in which the swollen micellar aggregates are assumed to be a separate "phase" in thermodynamic equilibrium with singly dispersed polymer and oil molecules in aqueous solution. Prior theoretical work has shown that the formation of a pure oil core at the center of the aggregate is less thermodynamically stable than a micelle core consisting of thoroughly mixed polymer and oil;[23] therefore, only aggregates of the latter type are considered in this model. Furthermore, intermicellar interactions are neglected and so the model is only strictly applicable to dilute solutions of swollen micelles. The mole fraction, X_{gj}, of aggregates containing g polymer molecules and j oil molecules is, therefore,

$$X_{gj} = X_1^{\,g} X_{1j}^{\,j} \exp\left(-\frac{g}{kT}\Delta\mu_{gj}^{\,0}\right) \tag{1}$$

$$\Delta\mu_{gj}^{\,0} = \frac{1}{g}\mu_{gj}^{\,0} - \mu_1^{\,0} - \frac{j}{g}\mu_{1j}^{\,0} \tag{2}$$

where X_1 and X_{1j} are the mole fractions of singly dispersed polymer and oil molecules, respectively, $\Delta\mu_{gj}^{\,0}$ is the change in chemical potential due to the addition of one polymer molecule to the aggregate, $\mu_1^{\,0}$ is the standard state chemical potential of a singly dispersed polymer molecule, $\mu_{1j}^{\,0}$ is the chemical potential of the oil in water, k is Boltzman's constant, and T is the temperature.

To simplify calculations, it has been assumed that the aggregates are monodisperse and so the characteristics of the swollen micelle at equilibrium may be obtained by minimizing the chemical potential with respect to the number of polymer and oil molecules in the aggregate

$$\frac{\partial}{\partial g}\left(\frac{\Delta\mu_{gj}^{\,0}}{kT}\right) = 0, \quad \frac{\partial}{\partial j}\left(\frac{\Delta\mu_{gj}^{\,0}}{kT}\right) = 0 \tag{3}$$

According to the theory of Nagarajan and Ganesh, the change in chemical potential due to aggregation is determined by seven components

$$\Delta\mu_{gj}^{\,0} = (\Delta\mu_{gj}^{\,0})_{\mathrm{PPO,dil}} + (\Delta\mu_{gj}^{\,0})_{\mathrm{PPO,def}} + (\Delta\mu_{gj}^{\,0})_{\mathrm{PEO,dil}} + (\Delta\mu_{gj}^{\,0})_{\mathrm{PEO,def}} + (\Delta\mu_{gj}^{\,0})_{\mathrm{loc}} + (\Delta\mu_{gj}^{\,0})_{\mathrm{int}} + (\Delta\mu_{gj}^{\,0})_{\mathrm{loop}} \tag{4}$$

in which $(\Delta\mu_{gj}^{\,0})_{\mathrm{PPO,dil}}$ is the change in chemical potential due to dilution of the PPO block with oil in the micelle core, $(\Delta\mu_{gj}^{\,0})_{\mathrm{PPO,def}}$ is due to the deformation of the PPO block in the core to meet the uniform concentration constraint, $(\Delta\mu_{gj}^{\,0})_{\mathrm{PEO,dil}}$ is due to the dilution of PEO with water in the micelle corona, $(\Delta\mu_{gj}^{\,0})_{\mathrm{PEO,def}}$ is due to the deformation of PEO in the corona, $(\Delta\mu_{gj}^{\,0})_{\mathrm{loc}}$ is due to the localization of the PPO−PEO junction at the core−corona interface, $(\Delta\mu_{gj}^{\,0})_{\mathrm{int}}$ is the change in chemical potential caused by the formation of the core−corona interface at which oil and water come into contact, and $(\Delta\mu_{gj}^{\,0})_{\mathrm{loop}}$ is due to the formation of a loop in the PPO block so that both PPO−PEO junctions of the triblock copolymer can be at the core surface. The expressions for each of these chemical potential terms have been derived in refs 12 and 22, thus, only the results are summarized below.

$$\frac{(\Delta\mu_{gj}^{\,0})_{\mathrm{PPO,dil}}}{kT} = N_{\mathrm{PPO}}\left[\frac{v_{\mathrm{PPO}}}{v_j}\frac{1-\phi_{\mathrm{PPO}}}{\phi_{\mathrm{PPO}}}\ln(1-\phi_{\mathrm{PPO}}) + \frac{v_{\mathrm{PPO}}}{v_{\mathrm{j}}}(1-\phi_{\mathrm{PPO}})\chi_{\mathrm{PPO},j}\right] - N_{\mathrm{PPO}}\left[\frac{v_{\mathrm{PPO}}}{v_{\mathrm{W}}}\frac{1-\phi_{\mathrm{PPO1}}}{\phi_{\mathrm{PPO1}}}\ln(1-\phi_{\mathrm{PPO1}}) + \frac{v_{\mathrm{PPO}}}{v_{\mathrm{W}}}(1-\phi_{\mathrm{PPO1}})\chi_{\mathrm{PPO,W}} + \left(\frac{\sigma_{\mathrm{PPO,W}}L_{\mathrm{PPO}}^{\,2}}{kT}\right)\frac{6}{\alpha_{\mathrm{PPO}}N_{\mathrm{PPO}}^{\,1/2}}\right] \tag{5}$$

where N_{PPO} is the number of propylene oxide segments in the block, v_{PPO}, v_j, and v_{W} are the molecular volumes of a PO segment, oil, and water, ϕ_{PPO} and ϕ_{PPO1} are the volume fractions of PPO in the micelle core and in the singly dispersed state, respectively, $\chi_{\mathrm{PPO},j}$ and $\chi_{\mathrm{PPO,W}}$ are the Flory−Huggins interaction parameters between PPO/oil and PPO/water, $\sigma_{\mathrm{PPO,W}}$ is the interfacial surface tension of PPO and water, L_{PPO} is the length of a propylene oxide segment, and $\alpha_{\mathrm{PPO}} = (6/\pi)^{1/3}N_{\mathrm{PPO}}^{\,-1/6}\phi_{\mathrm{PPO}}^{\,-1/3}$ is the chain expansion parameter of PPO (i.e., the difference between the unperturbed end-to-end PPO chain length and the length of the swollen PPO chain). The first two terms of eq 5 account for the enthalpy and entropy of mixing PPO and oil in the micelle core. The third and fourth terms represent the enthalpy and entropy of the PPO chain in the singly dispersed state that the chain leaves to join the aggregate, and the final term accounts for the disappearance of the PPO−water interface present in the singly dispersed state.

The change in chemical potential due to deformation of the PPO block is given by

$$\frac{(\Delta\mu_{gj}^{\,0})_{\mathrm{PPO,def}}}{kT} = \left[\left(\frac{3\pi^2}{40}\right)\frac{R^2}{(N_{\mathrm{PPO}}/2)L_{\mathrm{PPO}}^{\,2}}\right] - \left[\frac{3}{2}(\alpha_{\mathrm{PPO}}^{\,2}-1) - \ln\alpha_{\mathrm{PPO}}^{\,3}\right] \tag{6}$$

where R is the radius of the micelle core and all other variables are defined as in eq 5. This expression represents the difference in the configurational free energy of a single PPO chain confined to the micelle core and that of the PPO chain in aqueous solution. The first term of eq 6 accounts for the nonuniform deformation of the PPO necessary to achieve the homogeneous concentration of the core assumed in the model, and the second term represents the deformation of a singly dispersed polymer chain.

$$\frac{(\Delta\mu_{gj}^{\,0})_{\mathrm{PEO,dil}}}{kT} = N_{\mathrm{PEO}}\left[\frac{v_{\mathrm{PEO}}}{v_{\mathrm{W}}}\frac{1-\phi_{\mathrm{PEO}}}{\phi_{\mathrm{PEO}}}\ln(1-\phi_{\mathrm{PEO}}) + \frac{v_{\mathrm{PEO}}}{v_{\mathrm{W}}}(1-\phi_{\mathrm{PEO}})\chi_{\mathrm{PEO,W}}\right] - N_{\mathrm{PEO}}\left[\frac{v_{\mathrm{PEO}}}{v_{\mathrm{W}}}\frac{1-\phi_{\mathrm{PEO1}}}{\phi_{\mathrm{PEO1}}}\ln(1-\phi_{\mathrm{PEO1}}) + \frac{v_{\mathrm{PEO}}}{v_{\mathrm{W}}}(1-\phi_{\mathrm{PEO1}})\chi_{\mathrm{PEO,W}}\right] \tag{7}$$

Equation 7 takes into account the change in hydration of

(22) Nagarajan, R.; Ganesh, K. *Macromolecules* **1989**, *22*, 4312.
(23) Nagarajan, R.; Ganesh, K. *J. Chem. Phys.* **1993**, *98*, 7440.

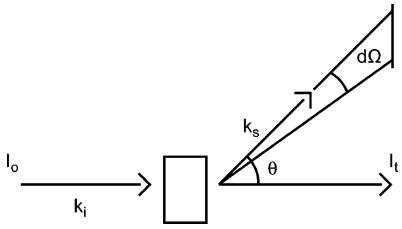

Figure 2. Neutron scattering geometery used in all SANS experiments. I_0 is the intensity of the incident neutron beam, I_t is the intensity of the transmitted neutron beam, k_i is the incident neutron wave vector, k_s is the scattered neutron wave vector, θ is the scattering angle, and Ω is the detector solid angle.

the PEO blocks of the polymer upon entering the micelle corona (first two terms) from its singly dispersed state (terms three and four).

$$\frac{(\Delta\mu_{gj}{}^0)_{\mathrm{PEO,def}}}{kT} = \left[\frac{3L_{\mathrm{PEO}}R}{(a/2)\phi_{\mathrm{PEO}}}\frac{D/R}{1+(D/R)}\right] - [3(\alpha_{\mathrm{PEO}}{}^2 - 1) - 2\ln \alpha_{\mathrm{PEO}}{}^3] \quad (8)$$

in which a is the area of the core surface occupied by each PEO block and D is the thickness of the micelle corona. The first term in eq 8 denotes the free energy of deformation of the PEO blocks in the micelle corona, while the second term represents the corresponding free energy of the PEO blocks in the singly dispersed state.

$$\frac{(\Delta\mu_{gj}{}^0)_{\mathrm{loc}}}{kT} = -2\ln\left[\frac{3L_{\mathrm{PEO}}}{R(1+D/R)^3}\right] \quad (9)$$

Equation 9 accounts for the entropic penalty paid by forming a micelle due to the localization of the PPO−PEO junction at the core−corona interface.

$$\frac{(\Delta\mu_{gj}{}^0)_{\mathrm{int}}}{kT} = \frac{a}{kT}[\sigma_{\mathrm{PPO,W}}\phi_{\mathrm{PPO}} + \sigma_{j,\mathrm{W}}(1-\phi_{\mathrm{PPO}})] \quad (10)$$

In eq 10, σ_{PPO} and $\sigma_{j,\mathrm{W}}$ are the surface tensions of PPO−water and oil−water, respectively. It is assumed that the volume fraction of PEO in the corona is very small and, therefore, that all oil and PPO at the core surface are exposed to water (leading to the σ_{PPO} and $\sigma_{j,\mathrm{W}}$ terms).

$$\frac{(\Delta\mu_{gj}{}^0)_{\mathrm{loop}}}{kT} = \frac{3}{2}\beta\ln(N_{\mathrm{PPO}}) \quad (11)$$

The final term in the model accounts for the backfolding in the central PPO block that is required so that both terminal PEO blocks can be in the corona. In this expression, β is an excluded volume parameter that is assumed to be unity.

Neutron Scattering Model

The neutron scattering configuration used for our experiments is shown in Figure 2. The neutron scattering intensity is reported as the neutron scattering cross section, σ, per unit solid angle, Ω, divided by the total sample volume, V.

$$I(q) = \frac{1}{V}\frac{\partial\sigma}{\partial\Omega} = \frac{\partial\Sigma}{\partial\Omega} \quad (12)$$

The overall neutron scattering cross section comprises two terms, the coherent (σ_{coh}) and the incoherent (σ_{inc}) scattering, so that $\sigma = \sigma_{\mathrm{coh}} + \sigma_{\mathrm{inc}}$. The change in the incoherent scattering of neutrons with the unit solid angle is constant, therefore, $\partial\sigma_{\mathrm{inc}}/\partial\Omega = C_{\mathrm{inc}}$ and

$$I(q) = \frac{\partial\Sigma_{\mathrm{coh}}}{\partial\Omega} + \frac{C_{\mathrm{inc}}}{V} \quad (13)$$

The differential coherent scattering cross section per unit volume for particulate samples can be expressed as the product of the number density of particles, an intraparticle form factor that accounts for the scattering from the atoms in a single micelle, $P(q)$, and an interparticle structure factor, $S(q)$, which accounts for the interactions between micelles.[24] Thus

$$\frac{\partial\Sigma_{\mathrm{coh}}}{\partial\Omega} = \frac{N_{\mathrm{p}}}{V}P(q)\,S(q) \quad (14)$$

where N_{p} is the total number of particles. Because we are working with very dilute solutions of swollen micelles, ~1−3 vol %, we assume that interparticle interactions are negligible and, therefore, that $S(q) \sim 1$. The intraparticle form factor may be expressed as the square of the Fourier transform of the neutron SLD spatial distribution.

$$P(q) = |F(q)|^2 = \left|\int_{\mathrm{particle}}[\rho(r) - \rho_{\mathrm{s}}]\exp(iqr)\,\mathrm{d}^3r\right|^2 \quad (15)$$

where $\rho(r)$ is the neutron SLD at position r and ρ_{s} is the SLD of the solvent.

Because the thermodynamic model for microemulsion formation assumes that the volume fractions of PEO in the corona and PPO in the core are homogeneous, the neutron SLD is, therefore, assumed to be constant within the core and the corona, such that

$$\rho(r) = \begin{cases} \rho_1 = \rho_{\mathrm{PPO}}\phi_{\mathrm{PPO}} + \rho_{\mathrm{oil}}(1-\phi_{\mathrm{PPO}}) & \text{for } 0 \le r \le R_1 \\ \rho_2 = \rho_{\mathrm{PEO}}\phi_{\mathrm{PEO}} + \rho_{\mathrm{water}}(1-\phi_{\mathrm{PEO}}) & \text{for } R_1 \le r \le R_2 \end{cases} \quad (16)$$

in which ρ_1 and ρ_2 are the SLDs of the core and the corona, respectively, and ρ_{PPO}, ρ_{PEO}, ρ_{oil}, and ρ_{water} are the SLDs of PPO, PEO, oil, and water, respectively. As above, ϕ_{PPO} is the volume fraction of PPO in the core and ϕ_{PEO} is the volume fraction of PEO in the corona. R_1 is the core radius, and R_2 is the corona radius (i.e., $R_2 = R_1 + D$, where D is the thickness of the corona).

Substituting eq 16 into eq 15, multiplying by the overall particle number density, and integrating, we obtain

$$I_{\mathrm{coh}}(q) = \frac{N_{\mathrm{p}}}{V}\left[\frac{4\pi}{3}R_1{}^3(\rho_1-\rho_2)\frac{3j_1(qR_1)}{qR_1} + \frac{4\pi}{3}R_2{}^3(\rho_2-\rho_{\mathrm{s}})\frac{3j_1(qR_2)}{qR_2}\right]^2 \quad (17)$$

where j_1 is a spherical Bessel function given by

$$j_1(x) = \frac{\sin(x) - x\cos(x)}{x^2} \quad (18)$$

Thus, eq 17 expresses the relation between the neutron intensity and the wave vector transfer for a suspension of noninteracting particles with cores of radius R_1 and uniform SLDs of ρ_1 and coronas of radius R_2 and SLD ρ_2. To fit the neutron scattering data with the neutron

(24) Chen, S.-H. *Annu. Rev. Phys. Chem.* **1986**, *37*, 351.

Table 1.

component, i	molecular volume, v (Å^3)	molecular length, $L = v^{1/3}$ (Å)	component i−water interfacial tension, σ_{iw} (J/Å^2)	solubility parameter, δ_i (MPa$^{1/2}$)	polymer−water interaction parameter, χ_{iw}
PPO	96.5	4.6	2.6×10^{-22}	19	2.1
PEO	64.6	4.0	8.0×10^{-23}	20.2	0.2
TMB	232.0	6.1	3.6×10^{-22}	18.4	
DCB	187.0	5.7	3.2×10^{-22}	20.5	
water	30.0	3.1			

scattering model, we used a nonlinear least-squares fitting algorithm that was developed at NIST.[25] The fitting parameters used in this algorithm are the volume fraction of particles, ϕ, which is used to determine N_p/V, the average core radius, R, the corona thickness, D, the core SLD, ρ_1, the corona SLD, ρ_2, the solvent SLD, ρ_s, the incoherent background, and the core dispersity, p. The polydispersity of the micelle cores was expressed using the normalized continuous Schultz distribution, $f(r)$.[26−28]

$$f(r) = (z + 1)^{z+1} x^z \exp[-(z + 1)x]/\bar{r}\Gamma(z + 1) \quad (19)$$

in which $\bar{r}$ is the mean core radius, $x = r/\bar{r}$, and $z = (1 - p^2)/p^2$, where the polydispersity is defined as $\rho = \sigma/\bar{r}$ and σ^2 is the variance of the distribution. Including a polydisperse core in the model alters the form factor such that the size average form factor is given by[27]

$$P(q)\,\overline{F^2(q)} = \int f(r)\,F^2(qr)\,\mathrm{d}r \quad (20)$$

Results and Discussion

The overall SANS fitting procedure described in eqs 12−20 utilizes eight fitting parameters: the core diameter, the corona thickness, the SLD of the core, the SLD of the corona, the SLD of the solvent, the total volume fraction of particles, the core polydispersity, and the incoherent scattering background. To ensure the physical significance of our data fits, we have employed the thermodynamic model (equations 1−11) to predict a priori as many variables as possible.

The micellar core radius, corona thickness, volume fraction of PPO in the core (leading to the core SLD), and volume fraction of PEO in the corona (leading to the SLD of the corona) were all calculated from the thermodynamic model using an iterative process to minimize the free energy of the system according to eqs 1−11 and the molecular parameters provided in Table 1. Because each of our samples was made with a fixed oil-to-polymer mass ratio, the number of oil molecules per molecule of polymer in the aggregate was fixed. We then chose an aggregation number (g) and a corona thickness (D). From the aggregation number, the number of oil molecules in the core (j) could be calculated using the fixed ratio assumption. The total volume of oil and PPO in the aggregate could then be used to calculate the volume of the micellar core, and the core volume was in turn used to calculate the core radius. The core radius and the corona thickness were then used to determine the volume of the corona and, from that, the volume fraction of PEO in the corona. The choices of aggregation number and corona thickness were varied until the minimum free energy was found for the given oil type and concentration.

Table 2. SLDs for Contrast-Enhanced and Contrast-Matched Samples

sample type	water SLD (Å^{-2})	polymer SLD (Å^{-2})	oil SLD (Å^{-2})
contrast-matched TMB	4.7×10^{-7}	4.7×10^{-7}	6.0×10^{-6}
contrast-enhanced TMB	5.9×10^{-6}	4.7×10^{-7}	6.0×10^{-7}
contrast-matched DCB	4.7×10^{-7}	4.7×10^{-7}	4.8×10^{-6}
contrast-enhanced DCB	4.7×10^{-6}	4.7×10^{-7}	4.8×10^{-6}

The SLD of the solvent was controlled in our experiments by mixing H_2O and D_2O in known ratios. A SLD of 4.7×10^{-7} Å^{-2} was used for both PEO and PPO blocks of the polymer, and this information along with the known SLD of water and oil and the volume fractions of polymer in the core and corona calculated by the thermodynamic model was used to determine the SLD of the core and corona. Thus, the SLD of the solvent, corona, and core were determined a priori and were not used as fit parameters for the neutron scattering data.

The total volume fraction of micelles was calculated as the total volume of polymer and oil added to the solution (accounting for the concentration of singly dispersed polymer and oil molecules determined from the known solubilities of the compounds) divided by the total volume of the sample. The incoherent scattering background was fitted to the constant neutron scattering intensity at high q, and did not contain any structural information. Therefore, its presence as a fitting parameter did not detract from the interpretation of the structural data. The core polydispersity was the only remaining fitting parameter.

The results of the thermodynamic model were applied to the neutron scattering model, and these curves were used to fit the neutron scattering data, initially with the core polydispersity as the only fitting parameter. These initial "model" fits to the neutron scattering data gave excellent results, and, subsequently, the core diameter and the corona thickness of the micelle were varied slightly to improve the accuracy of the fit and to obtain the "experimental" micellar dimensions. This procedure was used to fit scattering data from samples with the contrast increased between water and polymer through the addition of deuterated compounds to enhance the "core−shell" structure of the swollen micelles and also for samples in which the solvent had been contrast-matched to the polymer, in effect making the scattering from the corona negligible and reducing the "core−shell" structure of the micelles to that of a simple sphere consisting of a mixture of polymer and oil. The SLDs of the water, polymer, and oil components for contrast-enhanced and contrast-matched samples using TMB and DCB as the swelling agents are shown in Table 2. The model predictions of the most important parameters and the results of the most accurate "experimental" fits are summarized in Table 3.

The fits to both contrast-matched and contrast-enhanced samples using TMB and DCB as the swelling agents are shown in Figure 3. The accuracy of the fits to data from

(25) Klein, S. *Wavemetrics Igor Pro Macro*; National Institute of Standards and Technology: Gaithersburg, MD, 1998.
(26) Schultz, G. V. *Z. Phys. Chem.* **1935**, *43*, 25.
(27) Hayter, J. B. In *Physics of Amphiphiles − Micelles, Vesicles, and Microemulsions*; DeGiorgio, V., Corti, M., Eds.; North-Holland: Amsterdam, 1983.
(28) Bartlett, P.; Ottewill, R. H. *J. Chem. Phys.* **1992**, *96*, 3306.

Table 3.

oil type, mass ratio	$R_{experiment}$ (Å)	R_{model} (Å)	$R_{matched}$[a] (Å)	$D_{experiment}$ (Å)	D_{model} (Å)	polydispersity	ϕ_{PPO}[b]	ϕ_{PEO}[b]	g[c]	a[d] (Å^2)
TMB 0.10	70	71	60	20	23	0.15	0.86	0.25	190	333
TMB 0.20	76	77	67	20	22	0.15	0.75	0.25	211	351
TMB 0.34	85	85	73	20	22	0.15	0.64	0.25	247	371
TMB 0.53	100	95	93	18	22	0.15	0.53	0.24	287	399
TMB 1.05	100	115	95	18	20	0.18	0.37	0.23	347	481
DCB 0.22	65	69	68	20	22	0.15	0.86	0.26	177	340
DCB 0.55	82	84	85	20	22	0.15	0.64	0.24	232	380
DCB 1.06	110	98	103	18	21	0.17	0.47	0.23	277	436

[a] $R_{matched}$ is the radius of the micelle core experimentally determined from samples in which the SLD of the water has been matched to that of the polymer, rendering the corona undetectable. [b] Values for the volume fraction of PPO in the micelle core and PEO in the micelle corona were obtained from the thermodynamic model and used unchanged in the fitting of the SANS data. [c] g represents the polymer "aggregation number", that is, the total number of polymer molecules in one micelle. The polymer aggregation number was determined using the model. [d] a is the core surface area per polymer molecule, and the values listed were obtained from the model.

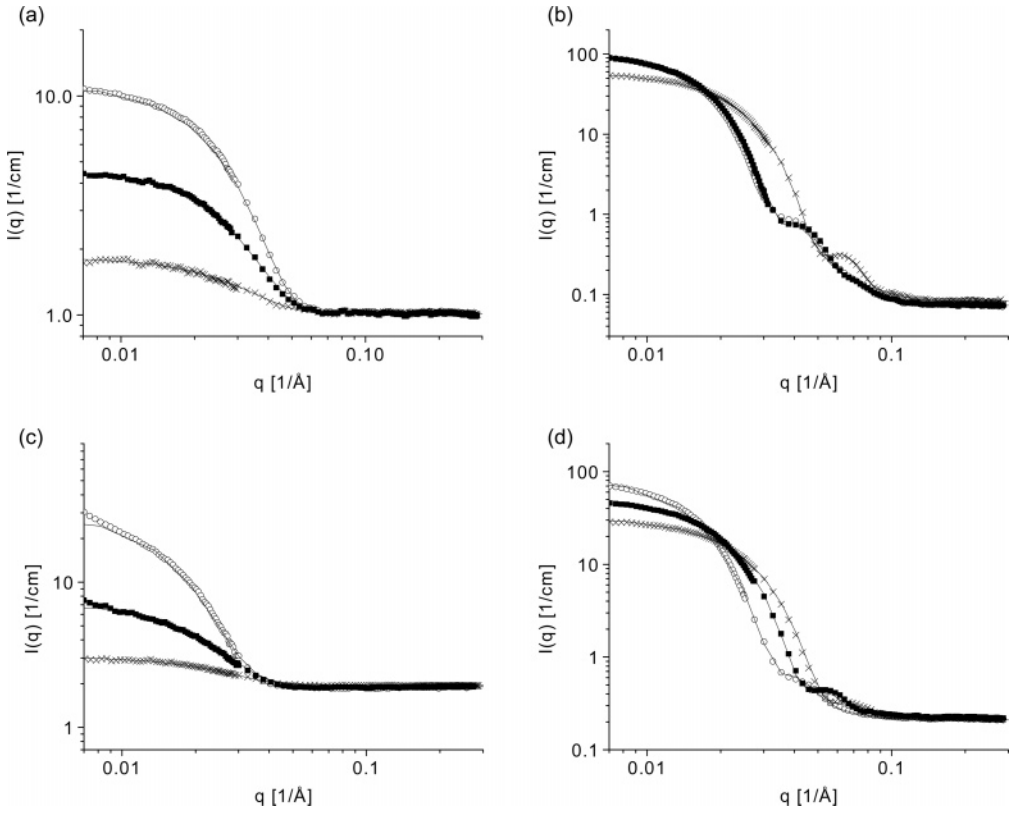

Figure 3. Neutron scattering data (symbols) and most accurate data fits (solid curves) for (a) samples containing TMB in which the neutron SLD of the water has been matched to that of the polymer, TMB-to-polymer mass ratios of (○) 0.34, (■) 0.20, and (×) 0.10; (b) samples containing TMB in which the contrast between water and polymer has been enhanced to clarify the "core−shell" micelle structure, TMB-to-polymer mass ratios of (○) 1.05, (■) 0.53, and (×) 0.20; (c) contrast-matched samples containing DCB with DCB-to-polymer mass ratios of (○) 1.06, (■) 0.55, and (×) 0.22; and (d) contrast-enhanced samples containing DCB with DCB-to-polymer mass ratios of (○) 1.06, (■) 0.55, and (×) 0.22.

both contrast-matched samples (Figures 3a,c) and contrast-enhanced samples (Figure 3b,d) indicates that the approximations of a homogeneous mixture of oil and polymer in the core and of a homogeneous volume fraction of PEO in the corona are reasonable ones.

The accuracy of the thermodynamic model in predicting the micelle structure can be seen in Figure 4, in which the overall micelle diameter from the most accurate fits to the SANS data and the initial predictions from the model are plotted against the volume of oil added. Figure 4 and Table 3 show that the model provides a very good starting point for the data fit, predicting the micelle diameter to within 5% accuracy for oil-to-polymer mass ratios below 0.5. The thermodynamic model correctly predicts the monotonic increase in micelle diameter with increasing oil content, although the micelle diameter predicted by the model tends to increase slightly less rapidly with increasing oil content than is experimentally observed. Furthermore, dynamic light scattering (DLS) studies of the oil-swollen micellar solutions have been performed to provide an independent confirmation of the micelle polydispersities obtained from our fits to the neutron scattering data. DLS experiments showed that the polydispersities of our oil−polymer aggregates ranged from 10 to 19%, in good agreement with the neutron scattering polydispersities of 15−18% shown in Table 3. Thus, all of the structural fit parameters from the neutron scattering model have been either theoretically predicted or confirmed by an independent technique.

As seen in Table 3 for both TMB and DCB mass ratios of ~1.0, the model predictions become less accurate at high oil concentrations. This is expected for two reasons: first, polymer chains behave differently at high extensions, and second, oil-to-polymer ratios greater than 0.4 for TMB

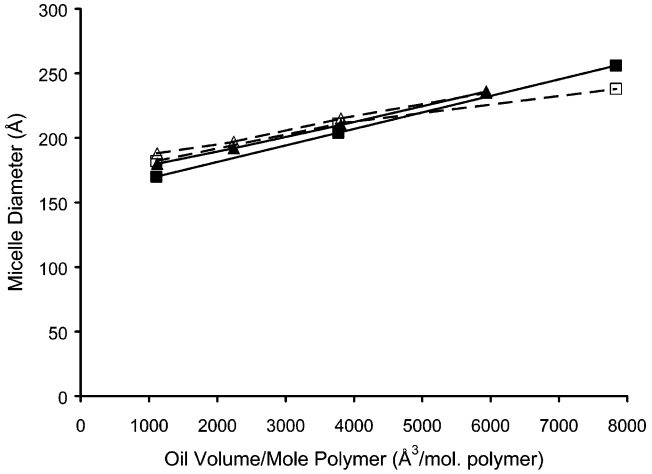

Figure 4. Micelle diameter determined from SANS experiments for samples containing TMB (▲) and DCB (■) and the micelle diameter from thermodynamic model predictions for TMB (△) and DCB (□) plotted against total volume of oil added per mole of polymer added. The lines are guides for the eye.

and 0.5 for DCB are above the microemulsion stability limit. The PPO blocks in the core become considerably extended as the core swells with oil. At the maximum oil/polymer ratio used in this study (TMB ∼ 1), the experimentally determined core diameter is 100 Å. It is assumed that the extended PPO block length is roughly equivalent to the core diameter because the PPO block must double over to ensure that both PEO blocks are in the corona. The contour length or end-to-end distance of the fully extended PPO block (NL) is ∼160 Å, and that of the unperturbed PPO block ($N^{1/2}L$) is ∼38 Å. Thus, the maximum observed extension is roughly 2/3 of the maximum extension and 3 times the unperturbed distance. It is noted by Kuhn and Grün[29] and by James and Guth[30] that the simple model of a freely jointed Gaussian chain must be modified at extensions beyond approximately 1/2 of the maximum. Furthermore, the PPO and PEO block deformation expressions given in eqs 6 and 8 do not limit the length of the blocks to their contour length and are, therefore, highly suspect at large extensions.

While the treatment of polymer chains at high extensions is one source of error at high oil contents, the transcendence of the microemulsion stability limit or cloud point is undoubtedly another. Above the cloud point, P123 solutions containing the oil phase segregate into a Windsor type I microemulsion (i.e., an oil-rich phase and an aqueous phase containing microemulsion droplets). The thermodynamic model was not intended to accurately predict the structure of swollen micelles beyond the phase separation point; however, it can offer important insight into the factors leading to the formation of a separate oil-rich phase. It has been shown in previous theoretical work that the oil solubilized by Pluronic surfactants does not form a separate oil core, and, therefore, the Pluronic−oil aggregates are most accurately described as swollen micelles rather than microemulsion droplets.[23] This trait means that the assumption of a homogeneous polymer−oil mixture in the core of the micelle is reasonable up to the phase separation point, but it also means that the size of the micelle core is limited by the contour length of the hydrophobic PPO block. Stretching the PPO block to reach the center of the micelle and, thus, preventing the formation of a pure oil core significantly decreases the entropy of the aggregate and, therefore, destabilizes the micelle. One way to solubilize more oil without further stretching the PPO block is to form smaller but more numerous micelles. The formation of more micelles, however, increases the overall core surface area and, hence, increases the core surface area per polymer molecule, a, listed in the last column of Table 3. The increase in a leads to increased oil−water interactions that also destabilize the swollen micelle and eventually lead to formation of a separate oil phase. As shown in Table 3, the model predicts that a steadily increases with increasing oil content and that the cloud point seems to be reached at a surface area per polymer molecule of ∼400 Å^2. The position of the microemulsion stability limit also explains why the neutron scattering data for samples with TMB/P123 of 0.53 and 1.05 shown in Figure 3b are nearly identical. The swollen micelles apparently do not grow after the cloud point has been reached with all of the additional oil going into the oil-rich phase.

The high solubilization capacity and selectivity of Pluronic surfactants for aromatic over aliphatic hydrocarbons has been noted.[31] This preference for aromatics is likely due to stronger dipole/induced dipole interactions between the permanent dipole of PPO and the more easily induced dipole of an aromatic relative to an aliphatic molecule. However, the greater polarity of DCB relative to TMB appears to have little effect on the volumetric solubility of the two compounds. As seen in Figure 4, the micelle diameters of DCB- and TMB-swollen samples are nearly identical at the same oil volumes. Small differences are noted in the aggregation number and surface area per polymer molecule of DCB- and TMB-swollen samples. The DCB-swollen samples have lower aggregation numbers and higher surface areas per polymer molecules than TMB-containing samples due to the more favorable interactions between DCB and water. A difference between DCB and TMB solutes is also present in the agreement between the core radii of contrast-matched samples (R_{matched}) and the radii of contrast-enhanced samples ($R_{\mathrm{experiment}}$). For DCB-containing samples, the agreement between R_{matched} and $R_{\mathrm{experiment}}$ in Table 3 is relatively good with R_{matched} tending to have the slightly higher value. In the case of TMB-containing samples, R_{matched} is consistently ∼10 Å lower than $R_{\mathrm{experiment}}$. This may be an indication that the TMB is not perfectly homogeneously distributed in the core and that the TMB concentration decreases close to the core−corona interface, again indicative of the poorer interactions of TMB and water compared to those between DCB and water.

In addition to studying the structure of the swollen micelles, we also investigated the effects of alcohols on the size and structure of the swollen micelles. In the first set of experiments, small amounts of ethanol were added to a solution of polymer in water. The addition of ethanol to the polymer solution immediately decreased the volume fraction of micelles in the solution, as seen in Figure 5, indicating that very small amounts of ethanol can act to increase the solubility of the singly dispersed polymer and, hence, reduce the micelle volume fraction. However, when the size of the pure polymer micelles is compared with the ethanol content, as in Figure 6, there is very little change in micelle diameter for the range of ethanol concentrations studied.

Neutron scattering data were also collected for micellar solutions containing TMB or DCB to which various amounts of ethanol had been added (see Figures 5 and 6).

(29) Kuhn, W.; Grün, F. *Kolloid Z.* **1942**, *101*, 248.
(30) James, H. M.; Guth, E. *J. Chem. Phys.* **1943**, *11*, 470.
(31) Nagarajan, R.; Barry, M.; Ruckenstein, E. *Langmuir* **1986**, *1*, 210.

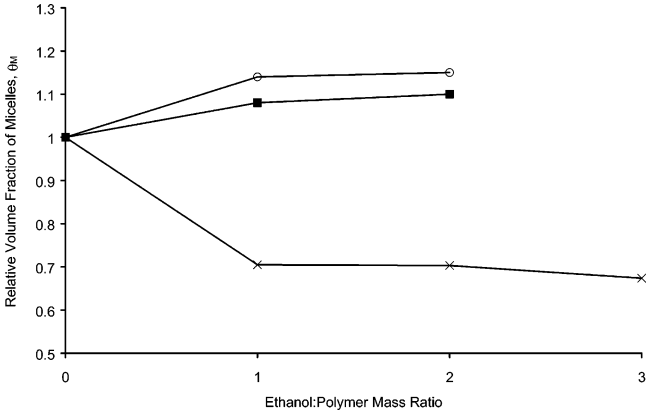

Figure 5. Volume fraction of micelles relative to the volume fraction at 0 ethanol content (θ_{M0}) plotted against the ethanol/polymer mass ratio for (○) TMB/polymer = 0.5, (■) DCB/polymer = 0.5, and (×) pure polymer. The relative volume fraction of micelles was determined from the absolute neutron scattering intensity at $q \approx 0$, $\sqrt{I_i(0)}/\sqrt{I_0(0)} \propto \theta_{Mi}/\theta_{M0}$. The Guinier method was used to correct $I(0)$ with respect to the radius of the micelles and for changes in contrast. The value of $I(0)$ for samples above the phase separation point was calculated by excluding the data below $q = 0.009$ from the Guinier plots, so that the second phase did not skew the $I(0)$ calculation.

The data in Figure 5 indicate that ethanol has a very different effect on oil-swollen micelles than on pure polymer micelles. Instead of decreasing the total volume fraction of micelles in the solution, as was seen for the pure polymer micelles, ethanol appears to increase the total volume fraction of oil-swollen micelles. It can be seen from Figure 6a that ethanol has very little effect on the size of the swollen micelles until phase segregation occurs at an oil-to-polymer mass ratio of ~0.4. After phase separation, the presence of ethanol appears to allow slightly larger micelles to form in the aqueous phase of type I microemulsion. As mentioned previously, one cause of swollen micelle destabilization is an increase in the surface area per polymer molecule with increasing oil content, which allows for a greater number of unfavorable oil−water interactions. Addition of ethanol to the solution decreases the oil−water surface tension and allows stable swollen micelles to form with slightly lower polymer surface concentrations. The effects of ethanol on the structure of DCB-swollen micelles were slight. It should be noted, however, that none of the DCB samples to which ethanol was added was significantly beyond the phase segregation limit.

Conclusions

There have been numerous studies exploring the structure of pure Pluronic micelles through the use of SANS, and there have been several theoretical attempts to describe the internal structure of Pluronic micelles swollen with oil. However, most of the theoretical models have been confirmed by comparing their predictions to experiments involving macroscopically observed phenomena, such as phase separation, while the models themselves can provide more rich and detailed information. We have compared the structural predictions of a thermodynamic model for the formation of Pluronic−oil aggregates, developed by Nagarajan and Ganesh,[12] to SANS data. We have found that the thermodynamic model accurately predicts the volume fraction of oil inside the micelle core and the volume fraction of water in the micelle corona and that the model estimates the size of the core and corona to within 5% of the experimental values. The success of the thermodynamic model in predicting the

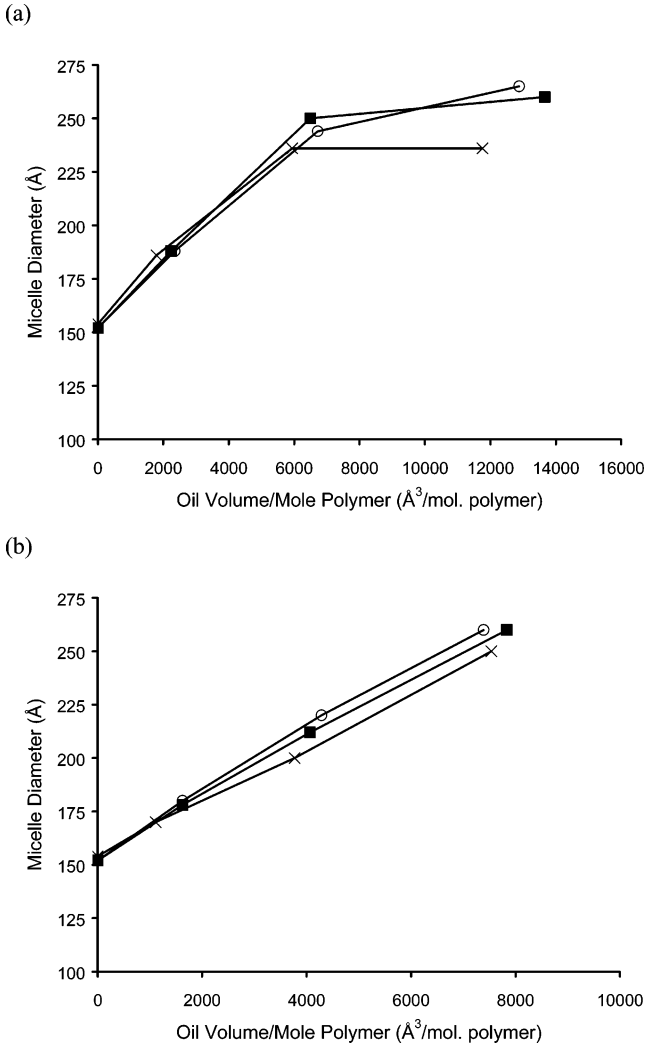

Figure 6. Micelle diameter determined from SANS experiments versus the volume of oil added per mole of polymer for samples with varying ethanol contents. (a) TMB as the solute and (b) DCB as the solute. Ethanol/polymer mass ratio = 2 (○), 1 (■), and 0 (×). Note that there is little change in the micelle diameter with changing ethanol concentration for samples that contain no oil.

internal structure of the swollen micelles is especially important, given the large number of parameters that would otherwise be required to fit the SANS data for this complex system. The good agreement between theory and experiment found in this work gives us a reliable structure for the swollen micelles. Knowledge of this structure will allow for more detailed understanding of important swollen micellar properties such as oil solubility, rheology, and inorganic material templating behavior.

The investigation of swollen micelles also included a study of the effects of alcohol on these systems. It was found that ethanol had little effect on the structure of the swollen micelles below the phase segregation limit, but that ethanol did appear to increase oil solubility, resulting in larger micelles above the phase segregation point. The thermodynamic model also gives us insight into the effects of ethanol on swollen micelles, and it is hypothesized that the greater oil solubility is a result of larger surface areas per polymer molecule made possible by the presence of ethanol.

Acknowledgment. We acknowledge the assistance of Mehul P. Shah and Todd C. Zion (M.I.T.) in the

preparation of samples and the acquisition of SANS data. We are grateful for comments and suggestions from Dr. Boualem Hammouda, Dr. Steven Klein, and Dr. Paul Butler (NIST). We also thank BASF for providing Pluronic P123 free of charge. This work was financially supported by the Singapore-MIT Alliance, and the Merk/M.I.T. Graduate Fellowship (J.S.L.). This study made use of the Center for Cold Neutron Research Facilities at the National Institute of Standards and Technology supported by the U.S. Department of Commerce and the National Science Foundation under Agreement No. DMR-9986442.

LA046918B